Scientia Iranica B (2016) 23(2), 566–574

Sharif University of Technology
Scientia Iranica
Transactions B: Mechanical Engineering
www.scientiairanica.com

Improvement of TFT-LCD's polarizer plate bubble problem using a preheating-process

Ch.-Sh. Lin[a,*], J.-T. Huang[a], P.Y. Wu[a], Y.-L. Lay[b] and H.-J. Shei[c]

a. *Department of Automatic Control Engineering, Feng Chia University, Taichung, Taiwan.*
b. *Department of Electronic Engineering, National Chin-Yi University of Technology, Taichung, Taiwan.*
c. *Department of Mechanical Engineering, China Institute of Technology, Taipei, Taiwan.*

Received 16 December 2013; received in revised form 22 April 2014; accepted 9 May 2015

KEYWORDS
Preheating-process;
Black matrix area;
Polarizer plate.

Abstract. In this study, improvement of the polarizer plate bubble in the thin film transistor liquid crystal display process, especially where the polarizer plate is attached to the black matrix area at the end of the glass substrate, is presented. This study proposed temperature control functions during the attaching process using the preheating operations of pressure sensitive adhesives and a pre-existing warp polarizer plate. The polarizer plate is softened evenly, and, then, the bubbles can be discharged smoothly in the attaching process. Three main control factors are used in the polarizer plate attachment process, using an experimental design method, to determine the best combination of parameters. By applying optimal parameters in the experiments, bubble width can be decreased by 60.49%, compared with that of the previous process.

1. Introduction

The polarizer plate is an undeniably important component in the production of the TFT (thin film transistor)-LCD (liquid crystal display). The TFT-LCD polarizer plate attaching process uses the attaching roller of a PU (Polyurethane) surface material to evenly attach the two polarizer plates onto the glass substrate [1]. Lin et al. listed many production defects that may occur which affect the performance of the LCD product [2]. In the LCD polarizer plate attaching process, the prevalent problem of bubbles between the glass substrate and the polarizer plate, due to uneven attachment, often causes quality deviations in the LCD of color image light leakage. Lin et al. proposed a method to evaluate the fracture and deformation status of conducting particles of anisotropic conductive film in the TFT-LCD assembly process [3]. Takatsuji and Arai found that holes in Al thin films will affect the TFT characteristics [4]. Jeong et al. proposed a simple method for computing production requirements for each step, where daily production demand is unknown [5]. Lin et al. found the types of TFT in TFT-LCD vary with different glass substrates; the pattern of each TFT is significantly different from its peripheral circuit wiring [6]. The reason for the polarizer plate process being hard to control is because the polarizer plate is a soft material, with a width of about $22 \sim 35$ μm, and, in the glass substrate process, the attached bubbles of the polarizer plate often result in a lack of optimization of the polarizer plate attaching process or polarizer plate curl. In particular, bubbles are easily observed in the BM (Black Matrix) areas at the start and end of the glass substrate, which cause product quality deviations. Hsieh proposed an integrated procedure incorporating data mining and stepwise regression techniques to achieve the construction of a yield loss model, the analysis effect of the manufacturing process and the clustering analysis of abnormal positions for TFT-LCD products [7].

*. *Corresponding author. Tel.: 886-4-24517250-3929; Fax: 886-4-24519951*
E-mail address: lincs@fcu.edu.tw (Ch.-Sh. Lin)

The instability of polarizer plate materials is mainly caused by multiple film stretching, curling, uncurling, attaching, and chemical processing, as well as dry and wet processes, which may easily lead to polarizer plate curl or wave curl, and, thus, seriously affect the quality of attachment. Othman et al. investigated the effect of the mechanical and thermal water absorption and morphological properties of bentonite filled polypropylene composites [8]. Polarizer plate curl measurement places the polarizer plate on a platform so that a steel ruler can be used to measure the heights between the 4 corner edges and the platform. The measurement, when the polarizing film is facing upward, is known as negative curl, while the measurement of the protective layer facing upward is known as positive curl. If the polarizer plate curls simultaneously with the protective layer and releases the film to form waves at the laterals, it is known as wave curl. The specifications of polarizer plate curls may vary from different polarizer plate suppliers. In terms of the mainstay 42″ TV products, the negative curl specification is $\leqq$ 15 mm, while positive curl specification is $\leqq$ 50 mm.

The curling of the polarizer plate in the attaching process is controlled by the attraction of the vacuum platform. However, the vacuum attraction will disappear instantly when the polarizer plate leaves the vacuum platform. In this case, the force that smoothens the polarizer plate is lost, and the polarizer plate contacts the glass substrate to result in air gaps within the glass substrate (Figure 1). Liu et al. used a plate-on-plate test rig to investigate the performance of the magnetorheological fluid-soaked metal foam setup [9]. Lee et al. proposed an integrated rolling model for computing thermo-mechanical parameters, such as the cross-sectional shape of the workpiece, the pass-by-pass strain, strain rate, and temperature variations during rolling and cooling between interstands [10]. Niculita found that maximum stress variation versus extension presents a short increase up to a maximum extension, and, from this peak value, this variation decreases in resin composite laminates [11]. Muliana and Lin proposed a multiscale formulation for analyzing coupled heat conduction and thermo-electro-mechanical deformation in heterogeneous active composites [12]. Philipp et al. considered that front end bending in plate rolling will reduce productivity eventually, entailing expensive downtime [13]. Anders et al. employed a dimensional analysis with the concept of physical similarity to derive dimensionless groups, which characterize the essential physics of the ski effect in rolling applications [14]. Grosman et al. used commercial Finite Element (FE) software to evaluate the rolling process parameters and analyze the character of material deformation, and compared them with experimental analyses performed on the developed prototype press [15].

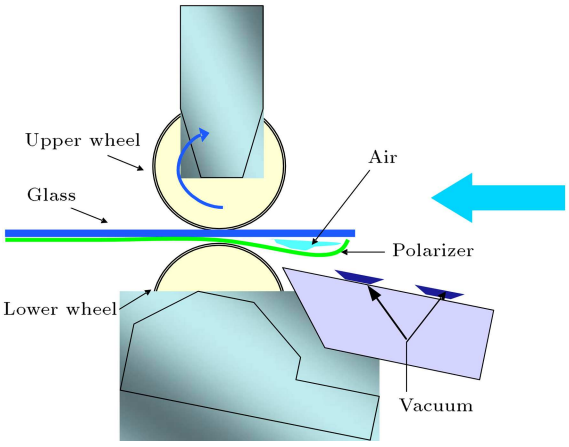

Figure 1. Polarizer plate attachment architecture.

The air inside the air gap cannot be expelled after being pressurized by the upper and lower attaching rollers, leading to BM bubbles. Since polarizer plate curling is a physical phenomenon, and the existing polarizer plate attaching processes employs the attaching roller, contact between the polarizer plate and the glass substrate cannot be prevented during the attaching process. Instead, only the distance between the vacuum sucker and the central line of the lower attaching roller can be shortened in order to reduce the frequency and level of attaching bubbles.

This study conducted an experimental design of attaching parameters by adding a preheated polarizer plate in the polarizer plate attachment to determine the optimal parameter combinations. By heating, the stress of the originally curled polarizer plate can be evenly released during attachment to shrink, evenly disperse, or eliminate the air inside the polarizer plate during the attaching process. This, thus, enhances the existing attached machinery process capability regarding curled polarizer plates.

2. Mathematical model of the stitching of the attaching process

The polarizer plate attachment is divided into two major sections: the glass substrate section and the polarizer platesection, both of which require position matching before attaching in the polarizer plate attaching section. Operations at the glass substrate side are as follows. A robot removes the substrate from the cassette and places it into the glass substrate panel cleaner in order to remove the particles from the substrate surface. The glass substrate rotates 180 degrees until the cross marks are matched, and then the glass substrate is moved to the attaching section of the polarizer plate. Operations at the polarizer plate side consist of a polarizer plate re-

mover and a polarizer plate cleaner, which conduct surface cleaning. When the positions of the polarizer plate corners are matched, the polarizer plate is moved to the polarizer plate attaching section in order to remove the released film. The glass substrate and polarizer plate require attaching at the CF and TFT sides before conducting an attachment accuracy test.

The stitching attachment process uses the upper and lower attaching rollers in the polarizer plate process, which belongs to the hot pitching process. In the following, this study will discuss how to control polarizer plate attachment speed, the attaching roller gap, and stitching temperature to improve the polarizer plate attachment thermal process. Using the hot pitching transformation model, as proposed by Avitzur [16], regarding distribution of the longitude vectors during the transformation process of the object [17], this study used polarizer plate attachment speed and temperature control to establish an appropriate mathematical model for stitching the polarizer plate attaching process [18-20].

As shown in Figure 2, Zone I ∼ Zone III represent different fields of speed, v_0 is the inlet speed of Zone I, v is the surrounding speed of Zone II stitching, v_f is the outlet speed of Zone III, t is the thickness of the polarizer plate before stitching, t_f is the thickness of the polarizer plate after stitching, α is the contact angle, R_0 is the radius of the stitching roller, and g is the attaching roller gap.

In Zone I, v is equal to v_0, and in Zone III, v is equal to v_f.

If the volume and speed remain unchanged, it can be defined as:

$$\frac{v_0}{v_f} = \frac{t_f}{t_0}. \tag{1}$$

From the geometry of Figure 2 and neglecting the attaching roller gap, g, the contact angle, α, can be computed as:

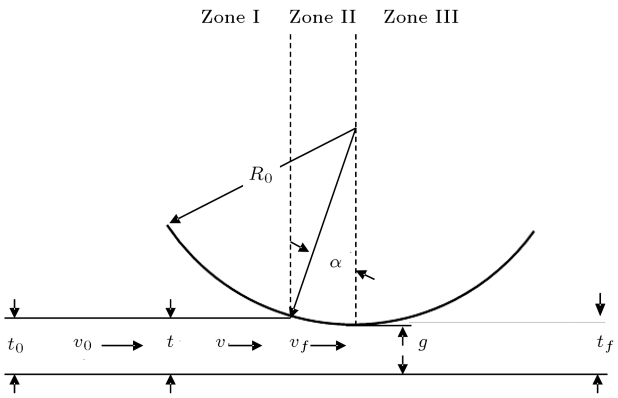

Figure 2. The assumed transformation model in the polarizer plate attaching process.

$$\alpha = \cos^{-1}\left(\frac{R_0 - (t_0 - t_f)}{R_0}\right) = \cos^{-1}\left(1 - \frac{t_0 - t_f)}{R_0}\right)$$

$$\approx \sqrt{\frac{t_f}{R_0}}\sqrt{\frac{t_0}{t_f} - 1}.$$

So, the function of contact angle α and attaching roller gap $f(g)$ can be defined as:

$$\alpha = f(g)\sqrt{\frac{t_f}{R_0}}\sqrt{\frac{t_0}{t_f} - 1}. \tag{2}$$

The thickness of the polarizer plate before stitching can be defined as:

$$t = t_f + 2R_0(1 - \cos\alpha). \tag{3}$$

Since the angle of α is extremely small, it can be rewritten into:

$$\sin\alpha \approx \alpha \quad \text{and} \quad \cos\alpha \approx 1 - \frac{\alpha^2}{2}.$$

$$t \approx t_f + R_0\alpha^2 = R_0\left(\frac{t_f}{R_0} + \alpha^2\right) = \left(1 + \frac{R_0}{t_f}\alpha^2\right).$$

In the given volume, the stitching speed is $\dot{U}$ and:

$$vt = v_f t_f = v_n t_n = \dot{U} t_n.$$

W_i is the shear force of unit width applied to represent the evenness of the attaching process of the polarizer plate, and can be defined as:

$$W_i = \sigma_0 t_f v_f \ln\frac{t_o}{t_f}. \tag{4}$$

σ_0 is the stress on the surface of the roller that can be applied as the attaching roller temperature function, represented by $f(T)$, and is defined as:

$$W_i = f(T) t_f v_f \ln\frac{t_o}{t_f}. \tag{5}$$

Since W_i and $f(T)$ are proportional, it indicates that the attaching roller temperature is a major factor in the improvement of the polarizer plate attachment evenness.

Jelali proposed that control performance assessment technology be used in industrial applications [21]. The settings of the specification central values of the various processes of Ca (capability of accuracy) expect deviation of the product central position, and can be regarded as the central value of the target. If the value is 0, there is no deviation. A greater value means a greater deviation, while a smaller value indicates smaller deviation. By comparison, as the unilateral specifications have no central values, Ca cannot be calculated. The standard equation of Ca is shown in Eq. (6):

Table 1. Ca rating and the relative handling rules.

Level	Ca value	Handling rules
A	$\|Ca\| \leqq 12.5\%$	Satisfying specifications and maintaining status
B	$12.5\% < \|Ca\| \leqq 25\%$	Requiring improvement to Level A
C	$25\% < \|Ca\| \leqq 50\%$	Reviewing the operational process for immediate improvement
D	$50\% < \|Ca\|$	Taking emergency measures and stopping production if necessary

Table 2. Cp rating and the relative handling rules.

Level	Cp value	Handling rules
A	$1.33 \leqq \|Cp\|$	Process is stable and tolerance can be reduced
B	$1.00 \leqq \|Cp\| \leqq 1.33$	Risk of producing defective products
C	$0.83 \leqq \|Cp\| \leqq 1.00$	Reviewing specifications and operating standards immediately
D	$\|Cp\| \leqq 0.83$	Taking emergency measures immediately for quality improvement

Table 3. Process capability indicator rating.

Level	C_{pk} value	Handling rules
A	$1.33 \leqq \|C_{pk}\|$	Process capability is adequate
B	$1.00 \leqq \|C_{pk}\| \leqq 1.33$	Process capability is sufficient but should be further improved
C	$\|C_{pk}\| \leqq 1.00$	The process should be improved

$$Ca = \frac{\bar{x} - u}{T/2} \times 100\%, \tag{6}$$

where $\bar{x}$ is the average value $(x_1 + x_2 + \cdots + x_n)/n$; u is the specification central value; and T is the specification tolerance, which is calculated by:

$$T = \text{USL} - \text{LSL},$$

in which USL is the Upper Specification Level of the characteristic value, and LSL is the Lower Specification Level of the characteristic value. If the product characteristic value is greater than USL, it is unqualified for engineering; if the product characteristic value is smaller than LSL, it is unqualified for engineering.

In Ca rating references, the smaller the Ca value, the better the quality. According to Ca values, Ca rating can be divided into four levels, as shown in Table 1.

In Cp (capability process), the setting of the upper and lower limits of various engineering specifications expects to enable the quality levels of a product to be in the tolerance range of the upper and lower limits, indicating the degree of consistency for process characteristics. The greater the Cp value, the more concentrated it will be, and will be more dispersed if the value is smaller. The standard equation of Cp is shown in Eq. (7):

$$Cp = \frac{T}{6\sigma} \text{ (bilateral specifications)}, \tag{7}$$

where σ is the process standard deviation estimate, i.e. the level of consistency of the current characteristic values of the process. When $T > \sigma$, the process is very suitable for precision production level of products. Cp reference for judgment is that when Cp is greater, it indicates stronger manufacturing capabilities of the factory, and that normal product distribution is more concentrated. Level determination and judgment can be divided into five levels, according to the values of Cp, as shown in Table 2.

The deviation and level of consistency should be taken into account, simultaneously. The standard equation is shown as follows:

$$C_{pk} = (1 - |Ca|)Cp. \tag{8}$$

Process capability indicator references for determination and judgment is that when the C_{pk} value is greater, it means the better comprehensive capability of the process. Level judgment and determination can be divided into five levels, according to the value of C_{pk}, as shown in Table 3.

3. Experimental data and results

With the Design Of the Experimental (DOE) method as the concept, this study discussed the impact of the attachment thermal process on polarizer plate BM bubbles, and determined the significant factors of the polarizer plate attaching process on the size of BM

Table 4. Major components of polarizer plate autoclaves.

Equipment description	Function and use
Stainless steel furnace Stainless steel furnace door	Pressurized autoclave furnace
Pressure gauge	Pressure detection: $0 \sim 6$ kg/cm^2
Temperature controller	Temperature detection: $0 \sim 80$°C
Stainless heating tube	Furnace heating
Cyclic fan	For even temperature of the furnace
Dry air inlet pipe	For increasing the pressure of the furnace
Dry air outlet pipe	For releasing furnace pressure
Transmission belt	Cassette input/output

bubbles. At the second stage, the ANOVA (analysis of variance) was applied to determine the contributions of the various factors, and their interactions in the polarizer plate attaching process, in order to obtain the optimal attaching parameters of the attachment thermal process. Chiang & Hsieh considered the correlation between quality characteristics and applied the principal component analysis to eliminate the multiple co-linearity [22]. At the third stage, the optimal attaching parameters of the attachment thermal process were introduced to compare BM bubble size with the original optimal parameters.

Autoclave uses air pressure and temperature to remove the attaching bubbles of the polarizer plate in a non-contact manner, with its main components as shown in Table 4. The equipment of a closed furnace structure was located after the polarizer plate attachment. The glass substrate attached to the polarizer plate was inputted into the furnace in the form of a cassette. After the furnace door was closed, the machinery pressed, according to set pressure and temperature parameters, to heat the temperature in the set range of 25°C∼70°C, and the pressure in the set range of $0 \sim 5 \times 10^4$ kg/(ms^2). The main manufacturing process principle was to speed up the flow of pressure sensitive adhesive by adjusting temperature and pressure parameters. Heating softened the pressure sensitive adhesive of the polarizer plate and the glass substrate to expel the BM bubbles from the edge of the polarizer plate. This was done by pressing, evenly dispersing, or removing the polarizer plate bubbles in the adhesive to improve the defects of the polarizer plate bubbles of the previous manufacturing processes.

This study verified the impact of temperature on BM bubble improvement levels, as well as the optimal parameters by autoclave parameter experiments. The above-mentioned polarizer plate pressure sensitive adhesive softening is an important condition for reducing or eliminating bubbles. Three factors affecting the contact area of the Pressure Sensitive Adhesive (PSA) are time, temperature, and pressure, which are the autoclave process parameters. Lin et al. obtained the optimal process conditions with the Taguchi methods, in order that alignment film printing can achieve the best product quality at the lowest cost [23]. Lakshminarayanan & Balasubramanian determined the optimum levels of process parameters using the Taguchi method to find the significant parameters in deciding the main process [24]. PSA is a viscous fluid characterized by flowability, and rising temperature can enhance the viscosity of the adhesive and increase its flow to enhance attachment opportunities with the surface. The pressure can enhance glue flow speed and eliminate bubbles in order to reduce the contact area between the bubble adhesive and the object.

To determine optimal conditions, this study conducted nine groups of experiments, with results shown in Figure 3. From the autoclave parameter main effects plotting and the autoclave parameter interactions plotting, the impact of the main effects of all factors, and interactions between factors can be understood.

As shown in the main effects plot, Factor A (autoclave pressure) and Factor B (autoclave temperature) have a significant impact on the reduction of the polarizer plate bubble width. When the temperature is above 50°C, the response value is better. When the pressure is above 4×10^4 kg/ms^2, the response value tends to become even. Regarding the interactions, Factors A and B have none of significance. According to the main effects and interactions plots, temperature has a greater influence than pressure in the polarizer plate pressurized bubble eliminating process. The optimal parameters can be defined as pressure above 4×10^4 kg/ms^2 and temperature above 50° C.

The experimental results showed that an autoclave temperature higher than 50°C is an important condition to improve polarizer plate attachment bubbles. If temperature control can be introduced in the attachment equipment to allow the temperature to

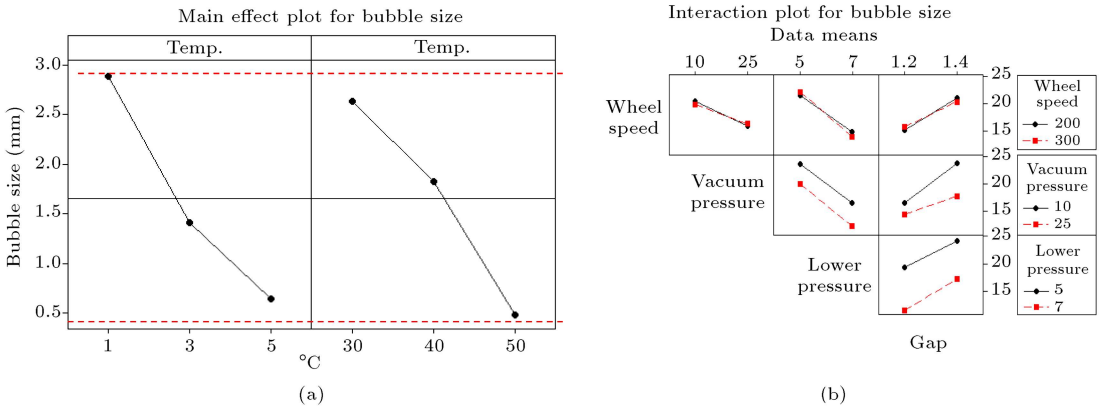

Figure 3. (a) Autoclave main factor affects. (b) Autoclave factor interaction effects.

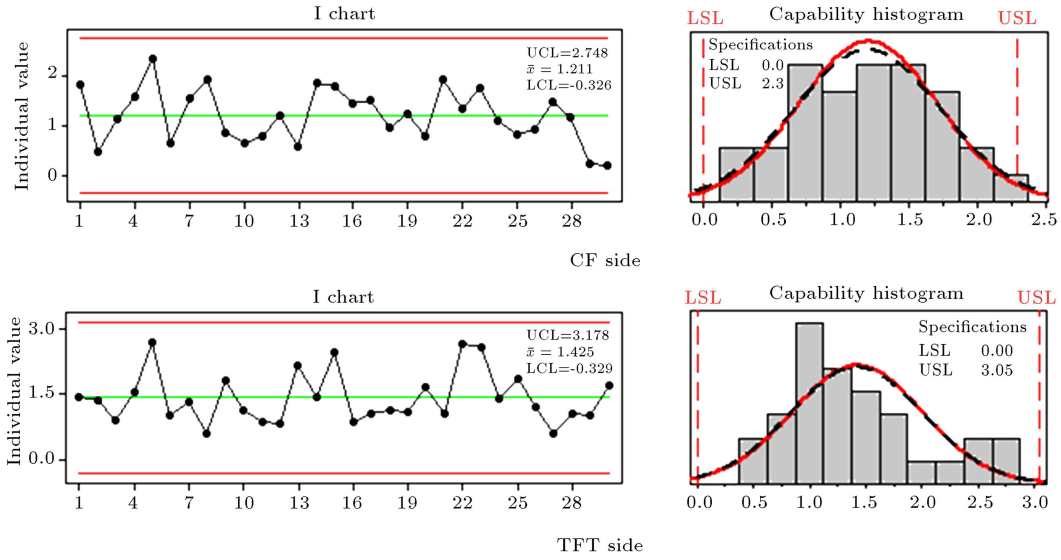

Figure 4. $42''$ product process control diagram.

become a parameter, it can reduce the opportunity to generate attachment bubbles.

By using bubble width collection values, according to the equation, the existing process capability value can be obtained. The MAX value is the maximum value of the collected values; the MIN value is the minimum value of the collected values; the AVG value is the average value of the collected values; the STD value is the standard deviation of the collected values; the Cp value is the Ca value of the collected values; and the C_{pk} value is the comprehensive process capability index of the collected values. Before improvement, the average value of the BM bubble width at the CF side was 1.183 mm, standard deviation was 0.5, and the process capability indicator was $C_{pk} = 0.51$ and $Cp = 0.69$. At the TFT side, the average value was 1.541 mm, standard deviation was 0.622, and the process capability indicator was $C_{pk} = 0.8$ and $Cp = 0.81$, as shown in Table 5. As shown in Figure 4, the existing BM bubble process capability remains unstable.

Table 5. $42''$ product process capability values.

Position	Max	Min	Avg	STD	Cp	C_{pk}
CF side	2.414	0.22	1.183	0.504	0.69	0.51
TFT side	2.706	0.613	1.541	0.622	0.81	0.8

The general problem-solving process can be divided in 5 steps:

Step 1: Define the target as: The width of the BM bubble from the glass substrate edge after improvement should be better than the existing process capability, and the average value should be smaller than 2.3 mm as smaller the better quality characteristic can obtain optimization and stability attaching parameter configuration.

Step 2: Conduct the attachment thermal process to verify BM bubble improvement, confirming that attachment thermal process is a major factor of the BM bubble.

Step 3: In the polarizer plate attaching process, de-

termine the factors and their level ranges influencing the polarizer plate BM bubble.

According to practical production experience, eight important factors are as follows:

1. Attachment gap: $0.8 \sim 1.6$ mm;
2. Attachment pressure: $0.3 \sim 0.8 \times 10^6$ kg/ms^2;
3. Attachment speed: $350 \sim 150$ mm/sec;
4. Weak vacuum pressure: $-10 \sim -40 \times 10^3$ kg/ms^2;
5. Attaching roller surface hardness: fixed at 70 degrees;
6. The attaching angle between the polarizer plate and glass substrate: 10∼15 degrees;
7. Position of the vacuum sucker at the attaching end: fixed at a distance of 4.6 cm from the center of the lower attaching roller;
8. The heating attaching roller and the platform temperature: $50 \sim 70$°C.

Step 4: Arrange the experiments to select important factors to establish a 2^k (non-repetitive) full-factor experimental design to collect data and obtain the minimum BM bubble width under all condition combinations.

Step 5: At the first stage of the experiments, apply ANOVA to calculate the contributions of various factors affecting BM bubble width, and identify the interactions between factors using the main effects and interaction plots. Use an ANOVA optimization model to determine the process parameters' optimal configuration.

Step 6: At the second stage of the experiments, add the two temperatures of the attaching roller into the process optimal parameters obtained at the first stage for actual production verification; collect BM bubble width data to determine the improvements of BM bubbles after the addition.

The bubble width collected values, as shown in Table 6, were used to calculate the existing process capability values. After inputting the process capability values into the BM bubble width of the attaching machine under optimal combination conditions, it was found that the average value at the CF size is 0.551 mm, standard deviation is 0.112, and the process capability indicators are $C_{pk} = 1.62$, $Cp = 3.38$. At the TFT, the average value is 0.497 mm, the standard deviation is 0.101, and the process capability indicators are $C_{pk} = 1.64$, $Cp = 5.03$. It was concluded that introduction of the optimal attaching parameters of the attachment thermal process can reduce BM bubble width by 53.42% at the CF side, and by 67.75% at the TFT side (Figure 5), suggesting that the attachment thermal process can substantially increase polarizer plate attachment process capability (Figure 6). By applying the optimal parameters in experiments, the average bubble width can be decreased by 60.49%, as compared with that of the previous process.

4. Conclusions

The key factors of the experiment are the lower attaching roller temperature, the lower attaching support pressure and gap between the upper and lower

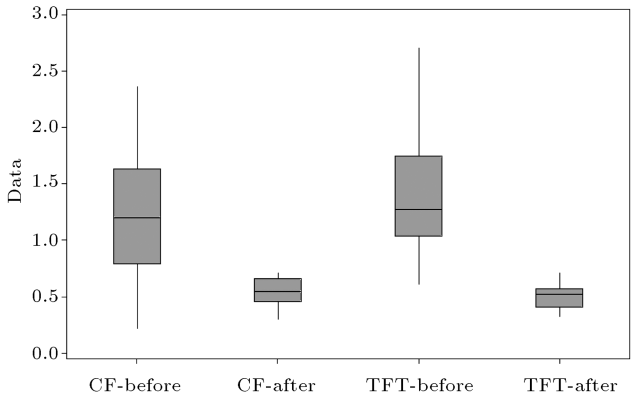

Figure 5. Box plot of $42''$ product before and after the incorporation of the optimal attaching parameters in the attachment thermal process.

Table 6. $42''$ product's process capability values before and after the incorporation of the optimal attaching parameters in the attachment thermal process.

Comparison	Application	Average value (mm)	Standard deviation (mm)	Cp	C_{pk}	Improvement
(A)	Before	1.183	0.504	0.69	0.51	53.42%
	After	0.551	0.112	3.38	1.62	
(B)	Before	1.541	0.622	0.81	0.8	67.75%
	After	0.497	0.101	5.03	1.64	

(A) Comparison of BM bubble width values before improvement at the CF side.

(B) Comparison of BM bubble width values before improvement at the TFT side.

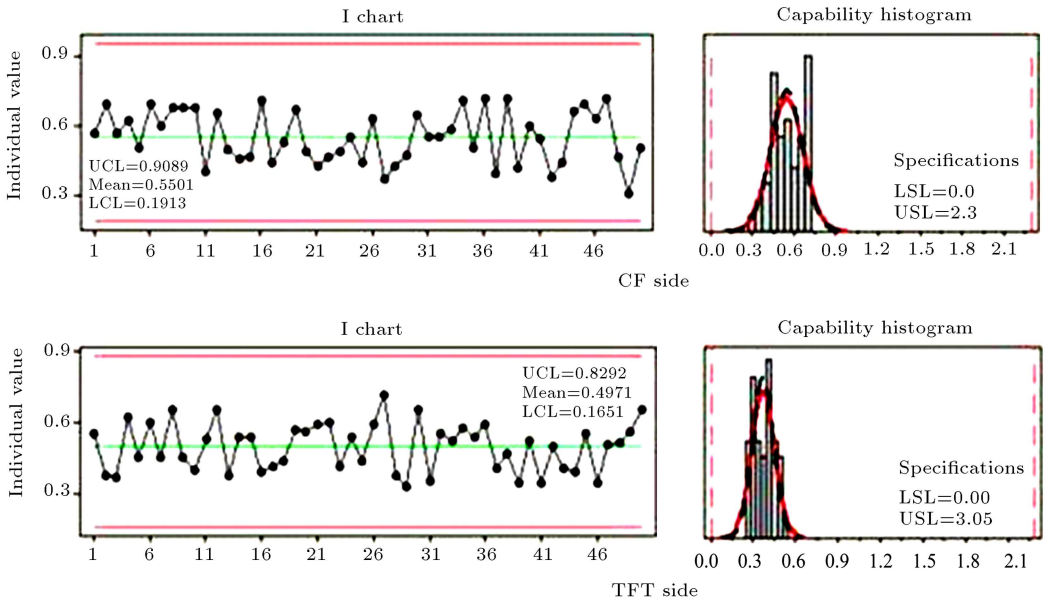

Figure 6. Process control diagram after the incorporation of the optimal attaching parameters into the attachment thermal process.

attaching rollers, and the attaching end's weak vacuum pressure. In this study, the uncontrollable factors included polarizer plate curling height, the attaching roller surface hardness, and the angle between the attaching polarizer plate and glass substrate. After the experimental design of controlled temperature and humidity at 23 ± 1°C, 55 ± 5% RH, it was confirmed that three factors, including lower attaching roller temperature, lower attaching pressure, and gap between the lower and upper attaching rollers, are the major factors affecting polarizer plate BM bubble width. The optimal parameters are lower attaching roller temperature at 60°C, lower attaching pressure at 7×10^4 kg/ms^2, and the gap between the upper and lower attaching rollers at 1.2 mm.

According to the experiments, the BM bubble width at the CF side was reduced from 1.183 mm to 0.551 mm, standard deviation was reduced from 0.504 mm to 0.112 mm, and BM bubble width, C_{pk}, was improved from 0.51 to 1.62. At the TFT side, the BM bubble width was reduced from 1.541 mm to 0.497 mm, standard deviation was reduced from 0.622 mm to 0.101 mm, and BM bubble width, C_{pk}, was increased from 0.8 to 1.64, proving that the experience could effectively reduce polarizer plate BM bubble width, and enhance the polarizer plate attachment process yield rate.

Acknowledgments

This research project was supported by the National Science Council, under Grant no. NSC 101-2221-E-035-039-MY2.

References

1. Hsieh, K.L. "Achieving yield construction and process analysis in TFT-LCD industry based on critical layers and areas", *Journal of Scientific & Industrial Research*, **66**(11), pp. 891-897 (2007).
2. Lin, C.S., Liao, Y.C., Lay, Y.L., Lee, L.C. and Yeh, M.S. "High-speed TFT LCD defect detection system with genetic algorithm", *Assembly Automation*, **28**(1), pp. 69-76 (2008).
3. Lin, C.S., Huang, K.H., Lin, T.C., Shei, H.J. and Tien, C.L. "An automatic inspection method for the fracture conditions of anisotropic conductive film in the TFT-LCD assembly process", *International Journal of Optomechatronics*, **5**(3), pp. 1-13 (2011).
4. Takatsuji, H. and Arai, T. "Pinholes in Al thin films: their effects on TFT characteristics and Taguchi method analysis of their origins", *Vacuum*, **59**, pp. 606-613 (2000).
5. Jeong, B., Kim, S.W. and Lee, Y.J. "An assembly scheduler for TFT LCD manufacturing", *Computers & Industrial Engineering*, **41**(1), pp. 37-58 (2001).
6. Lin, C.S., Wu, K.C., Lay, Y.L., Lin, C.C. and Lin, J.M. "An automatic temple generating method of the machine vision system in TFT LCD assembly and positioning process with genetic algorithm", *Assembly Automation*, **29**(1), pp. 41-48 (2009).
7. Hsieh, K.L. "Incorporating ANNs and statistical techniques into achieving process analysis in TFT-LCD manufacturing industry", *Robotics and Computer-Integrated Manufacturing*, **26**(1), pp. 92-99 (2010).
8. Othman, N., Ismail, H. and Mariatti, M. "Effect of compatibilisers on mechanical and thermal properties of bentonite filled polypropylene composites", *Polymer Degradation and Stability*, **91**, pp. 1761-1774 (2006).

9. Liu, X.H., Wong, P.L., Wang, W. and Bullough, W.A. "Feasibility study on the storage of magnetorheological fluid using metal foams", *Journal of Intelligent Material Systems and Structures*, **21**(12), pp. 1193-1200 (2010).
10. Lee, Y., Choi, S. and Hodgson, P.D. "Integrated model for thermo-mechanical controlled process in rod (or bar) rolling", *Journal of Materials Processing Technology*, **125-126**(9), pp. 678-688 (2002).
11. Niculita, C. "Mechanical behavior of epoxy 1050_GBX300L-1250 glass fabric laminates subjected to three-point bend tests", *Optoelectronics and Advanced Materials-Rapid Communications*, **6**(3-4), pp. 487-490 (2012).
12. Muliana, A. and Lin, C.H. "A multi-scale formulation for predicting non-linear thermo-electro-mechanical response in heterogeneous bodies", *Journal of Intelligent Material Systems and Structures*, **22**(8), pp. 723-738 (2011).
13. Philipp, M., Schwenzfeier, W., Fischer, F.D., Wödlinger, R. and Fischer, C. "Front end bending in plate rolling influenced by circumferential speed mismatch and geometry", *Journal of Materials Processing Technology*, **184**(1-3), pp. 224-232 (2007).
14. Anders, D., Münker, T., Artel, J. and Weinberg, K. "A dimensional analysis of front-end bending in plate rolling applications", *Journal of Materials Processing Technology*, **212**(6), pp. 1387-1398 (2012).
15. Grosman, F., Madej, L., Ziółkiewicz, S. and Nowak, J. "Experimental and numerical investigation on development of new incremental forming process", *Journal of Materials Processing Technology*, **212**(11), pp. 2200-2209 (2012).
16. Avitzur, B., *Metal Forming: Processes and Analysis*, McGraw-Hill, Second Ed., New York, pp. 437-451 (1968).
17. Leacock, A.G., McCracken, D., Brown, D. and McMurray, R. "Numerical simulation of the four roll bending process", *Journal: Materials and Manufacturing Processes*, **27**(4), pp. 370-376 (2012).
18. Ossia, S.A. and Soltani, B. "Finite element simulation of the warm deep drawing process in forming a circular cup from magnesium alloy sheet", *Scientia Iranica, Transactions B*, **20**(4), pp. 1213-1220 (2013).
19. Sloan, M.R., Wright, J.R. and Evans, K.E. "The helical auxetic yarn-A novel structure for composites and textiles, geometry, manufacture and mechanical properties", *Mechanics of Materials*, **43**(9), pp. 476-486 (2011).
20. Moziraji, Z.P., Azimi, A. and Hannani, S.K. "Analysis and modeling of building thermal response to investigate the effect of boundary conditions", *Scientia Iranica, Transactions B*, **20**(4), pp. 1269-1277 (2013).
21. Jelali, M. "An overview of control performance assessment technology and industrial applications", *Control Engineering Practice*, **14**(5), pp. 441-466 (2006).
22. Chiang, Y.M. and Hsieh, H.H. "The use of the Taguchi method with grey relational analysis to optimize the thin-film sputtering process with multiple quality characteristic in color filter manufacturing", *Computers, Industrial Engineering*, **56**, pp. 648-661 (2009).
23. Lin, C.S., Shih, S.J., Lu, A.T., Hung, S.S. and Chiu, C.C. "The quality improvement of PI coating process of TFT-LCD panels with Taguchi methods", *Optik*, **123**(8), pp. 703-710 (2012).
24. Lakshminarayanan, A.K. and Balasubramanian, V. "Process parameters optimization for friction stir welding of RDE-40 aluminum alloy using Taguchi technique", *Trans. Nonferrous Met. Soc. of China*, **18**(3), pp. 548-554 (2008).

Biographies

Chern-Sheng Lin received a BS degree from National Cheng Kung University, Taiwan, in 1982, an MS degree in Mechanical Engineering from the National Taiwan University, in 1987, and a PhD degrees in Optical Science from the National Central University, in 1994. He is currently Distinguished Professor in the Department of Automatic Control Engineering at Feng Chia University, Taiwan. His current research interests include pattern recognition, image processing, and human-machine interface design.

Jung-Ti Huang received an MS degree from the Department of Automatic Control Engineering, Feng Chia University, Taiwan, in 2012, and is currently designer of electronic control systems, and precise mechanical equipment for AUO companies.

Pin-Yi Wu received a BS degree from the Department of Automatic Control Engineering, Feng Chia University, Taiwan, ROC, in 2010, and is currently employed as a Designer of electronic control systems, precise mechanics, optics, electronics, and light equipment.

Yun-Long Lay received a PhD degree in Optical Science from the National Central University, Taiwan, ROC, in 1996, and is currently Professor and Vice President of National Chin-Yi University of Technology. His research interests include artificial neural networks, pattern recognition, and medical signal processing.

Hung-Jung Shei received the PhD degrees in Bio-Industrial Mechatronics Engineering from the National Taiwan University, Taiwan, ROC, in 1998. Now, He is a professor and the dean of Office of Academic Affairs of China University of Science and Technology. His research interests include optical design, and mechanical structure analysis.